

Excitations in disordered bosonic optical lattices

Michael Knap,* Enrico Arrigoni, and Wolfgang von der Linden
*Institute of Theoretical and Computational Physics,
Graz University of Technology, A-8010 Graz, Austria*
(Dated: February 23, 2024)

Spectral excitations of ultracold gases of bosonic atoms trapped in one-dimensional optical lattices with disorder are investigated by means of the variational cluster approach applied to the Bose-Hubbard model. Qualitatively different disorder distributions typically employed in experiments are considered. The computed spectra exhibit a strong dependence on the shape of the disorder distribution and the disorder strength. We compare alternative results for the Mott gap obtained from its formal definition and from the minimum peak distance, which is the quantity available from experiments.

PACS numbers: 64.70.Tg, 73.43.Nq, 67.85.De, 03.75.Kk

Interacting many-body systems with disorder are fascinating and challenging from both the experimental as well as the theoretical point of view. Understanding disordered bosonic systems has been of great interest ever since the pioneering works on the Bose-Hubbard (BH) model [1], which describes strongly interacting lattice bosons. Originally, the disordered BH model has been used to approximately describe various condensed matter systems, such as superfluid helium absorbed in porous media [2, 3], superfluid films on substrates [4], and Josephson junction arrays [5]. However, seminal experiments on ultracold gases of atoms trapped in optical lattices shed new light on interacting bosonic many-body systems, as these systems provide a *direct* experimental realization of the BH model [6, 7]. Intriguingly, these experiments allow to observe quantum many-body phenomena, such as the quantum phase transition from a superfluid to a Mott state [8]. The condensate of atoms can be driven across this phase transition by gradually increasing the laser beam intensity, which is directly related to the depth of the potential wells. There is a large experimental control over the system parameters such as the particle number or lattice depth, and in addition the parameters are tuneable over a wide range. While optical lattices provide a very clean experimental realization of strongly correlated lattice bosons, they can be used to study disordered systems on a very high level of control as well. Disorder can be added to the regular optical lattice by several techniques, such as by superposing additional optical lattices with shifted wavelength and beam angles [9–14], laser speckle fields [15–18], or including atoms of a different species acting as impurities [19].

The disordered BH model has been widely investigated in the literature. Most of the work has been devoted to study the phase transitions occurring in the disordered BH model [20–35]. At zero temperature the ground-state phase diagram depending on the chemical potential, the tunneling probability of the particles and the disorder

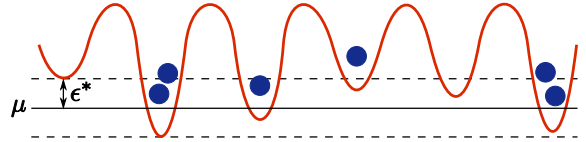


FIG. 1. (Color online) The periodic optical lattice potential is locally modified by disorder. In the illustration the disorder is bounded by ϵ^* corresponding to a situation obtained by the superposition of two incommensurate optical lattices.

strength, consists of three different phases: the Mott insulating, the superfluid, and the Bose glass phase. The first two phases are already present in the pure BH model, while the latter is a distinct feature of the disordered system. The Bose glass phase is characterized by being gapless and compressible, however, due to disorder the phase coherence does not extend over the entire system in contrast to the superfluid phase. While the phase diagram of the disordered BH model has been extensively studied, up to now spectral properties have not yet been investigated theoretically, even though they are experimentally accessible by Bragg spectroscopy, which allows to extract the wave vector dependent excitation energies of the system [36–38]. For low-energy excitations (typically $\omega/2\pi \lesssim 10\text{kHz}$) the response of the Bragg spectroscopy is ascribed to the structure factor, which corresponds to density fluctuations, whereas, for high excitation energies ($\omega/2\pi \gtrsim 30\text{kHz}$) the single-particle spectral function can be extracted [39, 40]. In this case, atoms excited into high-energy bands are not expected to interact with the lower bands. Therefore, the measured spectrum describes a convolution (without vertex corrections) of the density of states of the lower occupied with the upper unoccupied band. From this convolution the spectral function of the lower strong-correlated bands can be extracted [39].

In the present paper we study in detail the spectral properties of bosonic atoms in a disordered optical lattice, modeled by the one-dimensional BH model in which, for simplicity, the harmonic trap potential has been neglected. We focus on the strongly correlated regime and

* michael.knap@tugraz.at

evaluate spectral properties for the hopping strength to the on-site interaction ratio of size $t/U = 0.05$. This ratio corresponds to an optical lattice depth of $11 E_R$, where E_R is the recoil energy [41]. To evaluate this depth we considered laser beams with wave length $\lambda = 830 \text{ nm}$ and the scattering length of rubidium $a_s \approx 5 \text{ nm}$. In particular, we focus on the similarities and differences between the two common experimental methods used to induce disorder: (i) superposition of two laser fields with incommensurate wavevectors on the one hand, and (ii) the addition of a laser speckle field on the other hand. The disordered BH model and the disorder distributions generated by the two experimental methods are introduced in Sec. I.

We investigate the spectral properties of the disordered BH model numerically using the variational cluster approach [42]. In this work we present the first application of the variational cluster approach on disordered, interacting many-body systems. A description of the method is given in Sec. II. Our results on the excitations of the disordered BH model are presented in Sec. III. The crucial point about our investigations is that the two experimental approaches described previously produce disorder with rather different distributions leading, in turn, to different distributions of the spectral weight, as we show in Figs. (2) and (5). In addition, we present two results for the Mott gap. The first one, termed Δ , is obtained from the smallest excitation energy. This is, in principle, the formally correct version, but it is hard to determine experimentally. The second one, termed Δ^{mp} , is evaluated from the minimum peak distance in the spectral weight, which is the accessible quantity in experiments. The two quantities exhibit a different behavior as shown in Fig. 4. Finally, in Sec. IV, we conclude and summarize our work.

I. DISORDERED BOSE-HUBBARD MODEL

The Hamiltonian of the BH model with on-site disorder [1] is given by

$$\hat{H} = -t \sum_{\langle i, j \rangle} b_i^\dagger b_j + \frac{U}{2} \sum_i \hat{n}_i (\hat{n}_i - 1) + \sum_i (\epsilon_i - \mu) \hat{n}_i, \quad (1)$$

where the operators b_i^\dagger (b_i) create (annihilate) bosonic particles at lattice site i . The first sum in Eq.(1) is restricted to nearest-neighbor sites. The hopping strength is denoted as t , U is the on-site repulsion and μ stands for the chemical potential, which controls the total particle number $\hat{N}_p = \sum_i \hat{n}_i = \sum_i b_i^\dagger b_i$. The site-dependent random variable ϵ_i introduces disorder. In the following calculations and discussions we use the local interaction U as unit of energy.

One sample-configuration of disorder is denoted as $\eta = (\epsilon_1, \epsilon_2 \dots \epsilon_N)$, where N is the number of lattice sites. The disorder modifies locally the depth of the optical lattice, see Fig.1 for illustration. Random disorder

is distributed according to a given probability distribution function (pdf) $p(\eta)$, which has to satisfy the normalization condition $\int p(\eta) d\eta = 1$. The average of a quantity X_η with respect to the pdf $p(\eta)$ is given by $X_p \equiv \langle X \rangle_p = \int p(\eta) X_\eta d\eta$. We consider ϵ_i as identically and independently distributed random variables leading to $p(\eta) = \prod_{i=1}^N q(\epsilon_i)$, where $q(\epsilon_i)$ is a pdf describing the disorder generated in the experiment. Experimentally, there are two main ways of introducing disorder, corresponding to two different pdf's. On the one hand, superposing two incommensurate optical lattices yields a shifted β distribution as demonstrated in Appendix A. The distribution is bounded by a maximum disorder strength ϵ^* . This approach is used, for example, in the setup by Fallani *et al.* [10], where two laser beams with wave lengths $\lambda_1 = 830 \text{ nm}$ and $\lambda_2 = 1076 \text{ nm}$ are superposed. Since these two wave lengths are highly incommensurable the disorder can be regarded as truly random, see Ref. 9. Alternatively, disorder can be generated by superposing a laser speckle field [43, 44] to the regular optical lattice. In this case, one obtains an exponential distribution $q(\epsilon_i) = \theta(\epsilon_i) \exp(-\epsilon_i/\bar{\epsilon})/\bar{\epsilon}$ where $\bar{\epsilon}$ specifies the mean disorder strength [43, 44]. In our calculations the distribution is additionally shifted about its median $\bar{\epsilon} \ln 2$ to avoid modifications of the chemical potential due to disorder. The exponential distribution is asymmetric and unbounded and thus, strictly speaking, the Mott phase, which is controlled by the extrema of the distribution [23, 24, 31, 32] does not occur anymore. However, the goal of the present paper is to mimic the results of the experimental measurements, for which the effects of the tail of the distribution are too small to be observable. Therefore we introduce a cut off for the disorder distribution of $4\bar{\epsilon} \ln 2$. In other words, realizations far off the median are not considered.

II. VARIATIONAL CLUSTER APPROACH

We employ the variational cluster approach (VCA) to investigate the phase boundary and spectral properties of the disordered BH model. VCA has been originally proposed for fermionic systems by M. Potthoff *et al.* in Ref. [42] and has been extended to bosonic systems in Refs. [45–47]. The mathematical concept for the treatment of disordered systems by means of VCA can be found in Ref. [48]. In this paper we present the first application of VCA for disordered systems and on top of that, as a new contribution to VCA theory, we extend the so-called Q-matrix formalism [47, 49, 50] to a formulation suitable for disordered systems.

The basic concept of VCA is that the exact self-energy Σ_{ex} of a certain interacting system is given by the saddle point of a functional $\Omega[\Sigma]$, which becomes the exact grand potential at $\Sigma = \Sigma_{ex}$ [51, 52]. The important point is that the functional Ω can be computed exactly for a restricted set of self-energies associated with a so-called reference system, described by an Hamiltonian \hat{H}' , which

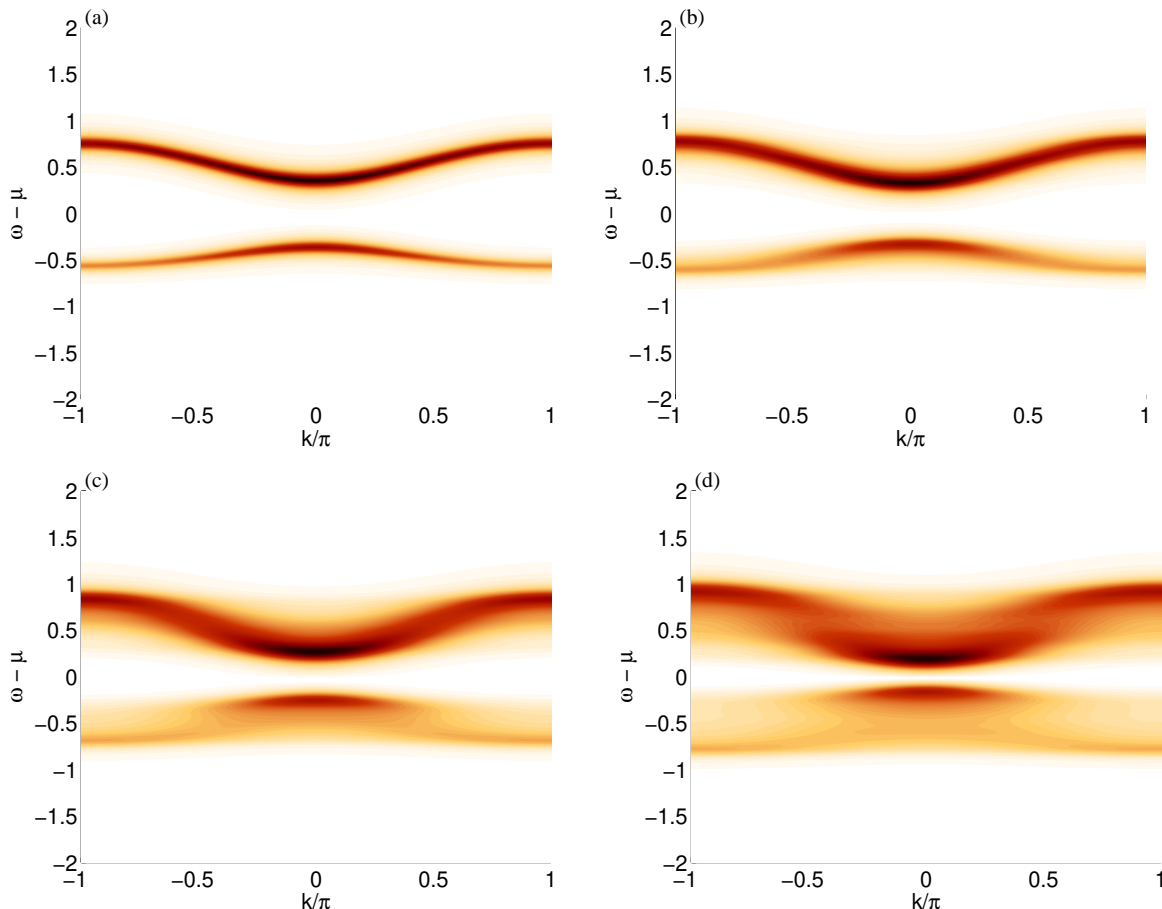


FIG. 2. (Color online) Spectral function $A_p(\mathbf{k}, \omega)$ for disorder generated by superposition of incommensurate optical lattices. The parameters are $t = 0.05$, $\mu = 0.45$, and (a) $\epsilon^* = 0.0$, (b) $\epsilon^* = 0.1$, (c) $\epsilon^* = 0.2$, and (d) $\epsilon^* = 0.3$.

shares its interaction part with the physical system. Typically, the reference system \hat{H}' is a decomposition of the physical system into independent clusters of a given size L , so that its Green's function can be determined numerically.

Disorder is treated by introducing a reference system which shares, in addition to the interaction part, the disorder distribution with the physical system. The expression for the averaged grand-potential within VCA then reads [48]:

$$\Omega_p = \Omega'_p + \text{Tr} \ln[-\mathbf{G}_p^{-1}] - \text{Tr} \ln[-\mathbf{G}'_p{}^{-1}], \quad (2)$$

where Ω'_p and \mathbf{G}'_p are the exact disorder averaged grand potential and Green's function of the reference system, respectively, which can be easily evaluated numerically with high accuracy. The averaged Green's function of the physical system reads $\mathbf{G}_p = (\mathbf{G}'_p{}^{-1} - \mathbf{V})^{-1}$, where $\mathbf{V} \equiv \mathbf{G}'_0{}^{-1} - \mathbf{G}_0^{-1}$, and \mathbf{G}_0 and \mathbf{G}'_0 are the noninteracting Green's functions of the pure physical and reference systems, respectively.

In Ref. [47] it has been discussed for a pure system that it is expedient for the evaluation of the traces in Eq. (2) to use the Q-matrix formalism. This formalism is based

on the Lehmann representation of the Green's function \mathbf{G}' of the reference system and that of the physical system \mathbf{G} . In the present paper, we extend the Q-matrix formalism to the case of disorder. For a specific disorder configuration η we have

$$\mathbf{G}'_\eta = \mathbf{Q}_\eta \mathbf{g}'_\eta \mathbf{S} \mathbf{Q}_\eta^\dagger, \quad (3)$$

where $\mathbf{g}'_\eta{}^{-1} = \omega - \Lambda_\eta$ and $(\Lambda_\eta)_{rr'} = \lambda_r^\eta \delta_{rr'}$ are the poles of the reference Green's function, see Ref. [47] for details. In praxis a specific number M of disorder configurations η (each consisting of L disorder realizations ϵ_i) has to be sampled to compute the average of a quantity X_η leading to $X_p \equiv \langle X \rangle_p \approx 1/M \sum_\alpha X_{\eta_\alpha}$. The averaged Green's function \mathbf{G}'_p thus reads

$$\mathbf{G}'_p = \frac{1}{M} \sum_\alpha \mathbf{G}'_{\eta_\alpha} = \frac{1}{M} \sum_\alpha \mathbf{Q}_{\eta_\alpha} \mathbf{g}'_{\eta_\alpha} \mathbf{S} \mathbf{Q}_{\eta_\alpha}^\dagger.$$

To exploit the Q-matrix formalism we write the averaged Green's function in a form similar to Eq. (3) and define

$$\mathbf{G}'_p \equiv \tilde{\mathbf{Q}} \tilde{\mathbf{g}}' \tilde{\mathbf{S}} \tilde{\mathbf{Q}}^\dagger,$$

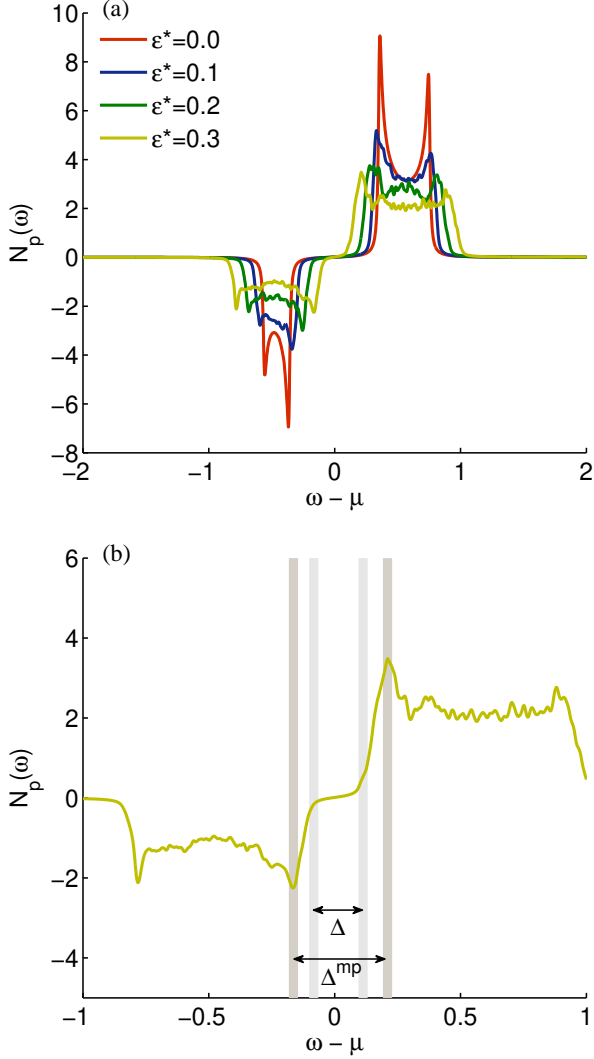


FIG. 3. (Color online) (a) Density of states $N_p(\omega)$ evaluated for the same parameters as in Fig. 2. (b) Illustration of the two “gaps” Δ and Δ^{mp} within a blowup of the the data for disorder strength $\epsilon^* = 0.3$. According to our definition (see text), Δ corresponds to the formal definition of the Mott gap based on minimal excitation energies, whereas Δ^{mp} corresponds to the minimum peak distance in the spectral weight, which is the quantity available from experiments.

where $\tilde{Q} \equiv (Q_{\eta_1}/\sqrt{M}, Q_{\eta_2}/\sqrt{M} \dots)$, $\tilde{S} \equiv \text{diag}(S, S, \dots)$ and $\tilde{g}' \equiv \text{diag}(g'_{\eta_1}, g'_{\eta_2}, \dots)$. With that we can proceed in the same way as for pure systems and write the averaged Green’s function of the physical system as

$$G_p = \tilde{Q} \frac{1}{\omega - (\tilde{\Lambda} - \tilde{S}\tilde{Q}^\dagger V \tilde{Q})} \tilde{S} \tilde{Q}^\dagger,$$

where $\tilde{\Lambda} \equiv \text{diag}(\Lambda_{\eta_1}, \Lambda_{\eta_2} \dots)$. By diagonalizing the matrix $M \equiv \tilde{\Lambda} - \tilde{S}\tilde{Q}^\dagger V \tilde{Q} = XDX^{-1}$ we obtain the poles D of the physical Green’s function and are thus able to evaluate the grand potential $\Omega_p(x)$.

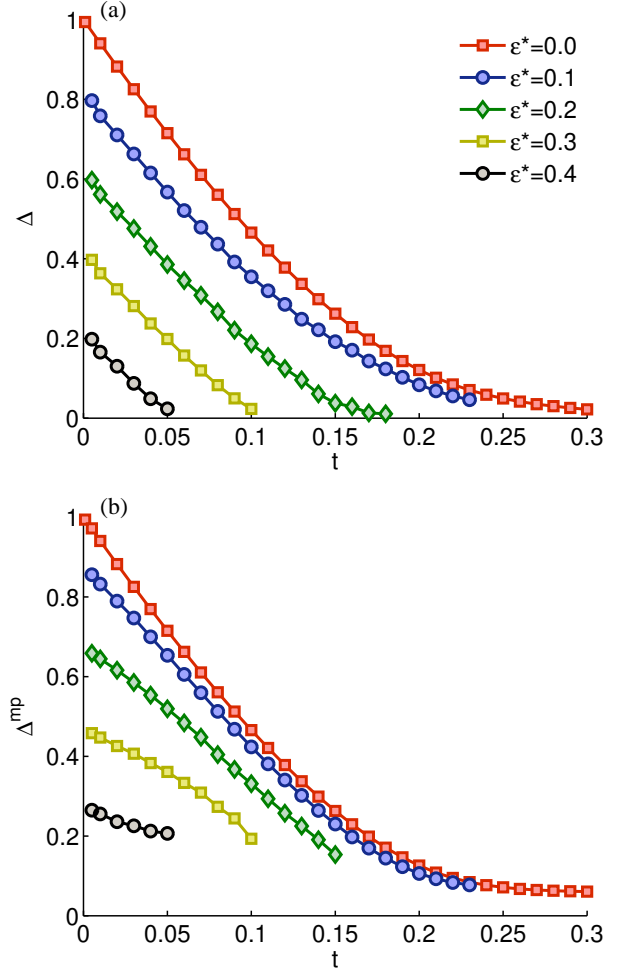


FIG. 4. (Color online) Gap Δ obtained from (a) the smallest excitation energies and (b) Δ^{mp} obtained from the minimum peak energy difference of the occupied and unoccupied bands.

III. RESULTS

We first investigate spectral properties for disorder realizations sampled from the shifted β distribution, which is realized experimentally by superposing two incommensurate optical lattices, see Appendix A for details on the distribution.

In particular, spectral functions $A_p(\mathbf{k}, \omega)$ are evaluated for hopping strength $t = 0.05$, chemical potential $\mu = 0.45$ and various strengths of disorder $\epsilon^* = \{0.0, 0.1, 0.2, 0.3\}$, see Fig. 2. The corresponding densities of states $N_p(\omega)$ are shown in Fig. 3.

For the numerical evaluation by means of VCA we use $M = 256$ disorder configurations, a reference system of size $L = 8$, and the VCA parameters $x = \{\mu, t, \delta\}$. The parameter δ is an additional on-site energy located at the boundaries of the cluster, whose introduction drastically improves the results, as shown in Ref. [53]. The artificial broadening parameter is chosen to be $0^+ = 0.05$ for spectral functions and $0^+ = 0.01$ for densities of states.

As mentioned in the introduction the occupied part of the single-particle spectral function is experimentally accessible by high-energy Bragg spectroscopy. For the pure system we obtain the well-known cosinelike shaped bands reminiscent of the dispersion of free particles on a lattice. For increasing disorder strength ϵ^* the minimal gap between the occupied and the unoccupied band shrinks. In addition, the bands become broader as the poles of the Green's function for a specific wave vector \mathbf{k} are distributed over a large energy range. This behavior can also be seen in the density of states. Furthermore, for large disorder the bands seem to split in two sections separated by a pseudogap around $k = \pi$. This is a peculiarity of this disorder configuration which to some extent resembles a binary distribution. An ordered binary distribution would double the unit cell thus producing a true gap at $k = \pi$.

Experimentally the gap Δ present in Mott phase can be determined for instance by lattice modulation [54] or by Bragg spectroscopy [36]. In these experiments the amount of energy transferred to the system is related to the width of the central peak observed in time of flight images [54]. The width of the central peak is measured for various energies leading to the excitation spectrum. Indeed for increasing disorder strength ϵ^* a broadening of the excitation band has been observed [10] which is qualitatively in agreement with our results for the spectral function. In addition, it could be shown experimentally that the weight moves to lower excitation energies for increasing ϵ^* [10]. However, it is rather difficult to extract the precise value of the gap from the measured excitation spectra. Strictly speaking, the gap Δ is defined as the energy difference of the lowest lying poles in the occupied and unoccupied bands, respectively. Yet, our results show, that these poles quite generally carry only very little spectral weight. This means that it is virtually impossible to detect them in the experiment. For this reason, it might be useful to introduce the notion of a gap Δ^{mp} , that corresponds to the experimental situation and is determined by the distance between the maxima of the spectral weight observed in the center of the Brillouin zone. In Fig. 4 we compare Δ [Fig. 4 (a)] with Δ^{mp} [Fig. 4 (b)] which is obviously always larger than Δ . For increasing hopping strength t the gap Δ^{mp} decreases, however, it still remains finite (i. e., $\Delta^{mp} \approx 0.2$) at values of t for which the gap Δ determined from the smallest excitation energies is already almost zero. Therefore, a peak at finite energy will be observed in the experimental data, even when the system is already in the Bose-glass phase. Additionally, it is important to mention that the smallest excitation energy gap Δ can be predicted analytically for systems with infinitely many disorder realizations. In this case Δ is controlled by the maximum disorder strength ϵ^* only. In particular, the phase boundary is shifted by $\pm\epsilon^*$ as there exist always rare regions where the chemical potential is either increased or decreased by ϵ^* [23, 24]. Here, however, we take into account a finite number of $LM = 2048$ random values for the on-site

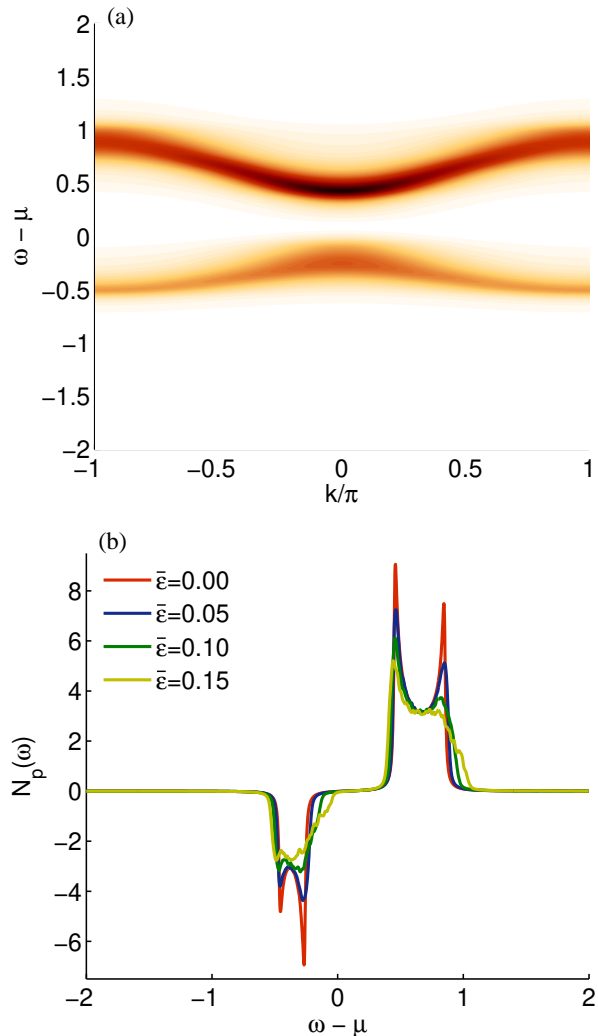


FIG. 5. (Color online) Spectral properties for a disorder distribution generated by laser speckle fields. The parameters are $t = 0.05$, and $\mu = 0.35$. Panel (a) shows the spectral function $A_p(\mathbf{k}, \omega)$ evaluated for $\bar{\epsilon} = 0.15$ and panel (b) shows the densities of states for various disorder strengths $\bar{\epsilon} = \{0.0, 0.05, 0.1, 0.15\}$.

energies ϵ_i leading to larger gaps, since it is very unlikely that all values ϵ_i of one realization η are close to the extreme cases $\pm\epsilon^*$. This resembles more closely the experimental situation in which only a limited number of disorder realizations can be detected.

The second kind of disorder we are addressing in this paper follows the shifted exponential distribution, which is generated by superposing a laser speckle field. Spectral properties of the Bose-Hubbard model for this disorder distribution are shown in Fig. 5. In contrast to the disorder realized by the superposition of two incommensurate optical lattices, the spectral signatures evaluated for the exponential distribution clearly exhibits an asymmetric shape. This becomes particular visible when comparing the densities of states for various disorder strengths, see

Fig. 5 (b). In particular, the poles are smeared out toward higher excitation energies and thus reflect the tail of the exponential distribution. No pseudogap behavior around $k = \pi$ is observed here, due to the shape of the exponential distribution which is in contrast to the β distribution not peaked at the edges.

IV. CONCLUSIONS

In the present work we investigated for the first time spectral properties of the disordered Bose-Hubbard model. In view of a realistic description of the experimental results, we focused on disorder distributions which are relevant for ultracold gases of atoms in optical lattices. In particular, we studied the differences between disorder realized by the superposition of incommensurate laser fields with the one obtained by laser speckle fields. In both cases we evaluated spectral functions and densities of states and showed that the resulting spectral weight strongly depends on the underlying shape of the disorder distribution. Furthermore, we determined the gap present in the Mott phase for disorder generated by incommensurate optical lattices. On the one hand, we evaluated the gap Δ from the minimal excitation energies of the system and on the other hand we determined the gap Δ^{mp} from the minimum peak distance in the spectral weight located at the center of the Brillouin zone. Whereas Δ cannot be observed directly in the experiment since the low-energy excitations carry very little spectral weight, Δ^{mp} is directly measurable. Furthermore, Δ^{mp} is always larger than Δ and thus Δ^{mp} remains finite even at the Mott to Bose-glass transition. In our calculations, we neglected the harmonic trap potential present in the experiments with ultracold gases of atoms. In principle, this effect can be included in our formalism, however, with a significantly major effort which goes beyond the goal of the present work. There are two cases in which neglecting the trap potential is justified. As in the ordered case, one can expect for sufficiently small disorder strength the trap potential to lead to multiple ringlike regions which are alternately Mott gapped and gapless. Quite generally, one should be able to choose the parameters so that the volume of the gapless regions is much smaller than the one of the $\hat{N}_p = N$ Mott region in which we are interested. In this case, the spectrum will display a nonvanishing weight within the gap originating from the gapless regions. However, we expect this to be small enough, at least for $\omega \neq 0$, so that the peaks defining the experimental gap Δ^{mp} remain discernible. Alternatively, spectroscopy experiments probing the system locally should be able to probe directly the Mott insulating region with no contributions from the gapless areas.

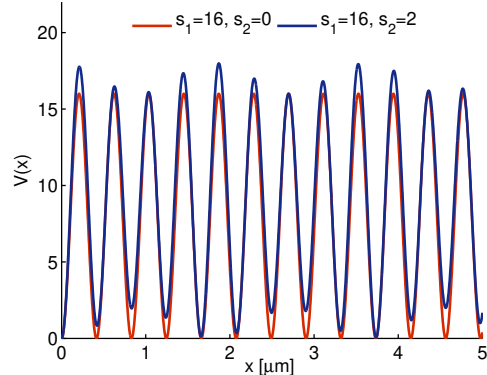


FIG. 6. (Color online) Total lattice potential created by the superposition of the main optical lattice with depth s_1 and the disorder lattice with depth s_2 .

ACKNOWLEDGMENTS

M.K. thanks P. Pippin for many useful discussions. We made use of parts of the ALPS library [55]. We acknowledge financial support from the Austrian Science Fund (FWF) under the doctoral program “Numerical Simulations in Technical Sciences” Grant No. W1208-N18 (M.K.) and under Project No. P18551-N16 (E.A.).

Appendix A: Disorder distribution generated by incommensurate optical lattices

In this Appendix we show that the potential distribution, which results from the superposition of two optical lattices, follows a shifted β distribution. In particular, we focus on the experimental setup of Fallani *et al.* [10], who used for the main optical lattice a laser at wavelength $\lambda_1 = 830$ nm. Disorder is generated by superposing an additional lattice created from a weak laser beam at $\lambda_2 = 1076$ nm. The resulting potential is given by

$$V(x) = s_1 E_{R1} \sin^2 2\pi x/\lambda_1 + s_2 E_{R2} \sin^2 2\pi x/\lambda_2 ,$$

where x is the spatial position, s_1 and s_2 are related to the depth of the potential generated from the laser beams at λ_1 and λ_2 , respectively. The constants E_{R1} and E_{R2} are the corresponding recoil energies. In this Appendix, the lattice depths s_1 and s_2 will always be stated in units of their recoil energies. The depth s_2 of the disorder-inducing wave is related to the maximal disorder strength ϵ^* by $\epsilon^* = s_2/2$. Since the wave lengths λ_1 and λ_2 are incommensurable the disorder imitates a true random behavior [9]. Here we reconstruct the histogram of the disorder distribution and find a mathematical expression, which reproduces the behavior of these physical systems.

In the experiments typical values for the lattice depths are $s_1 = 16$ and $s_2 = 2$, see Ref. [10]. Figure 6 compares

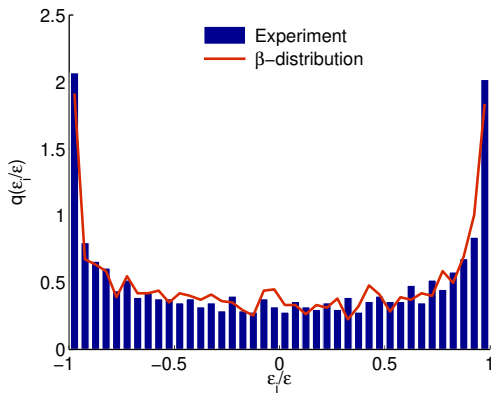


FIG. 7. (Color online) Distribution of the on-site energy ϵ_i observed in the experiment (histogram) compared with random samples drawn from the shifted β distribution (solid line).

the potential $V(x)$ for the previously mentioned values of $s_1 = 16$ and $s_2 = 2$ with the pure case, where the second laser beam at λ_2 is switched off, i. e., $s_1 = 16$ and $s_2 = 0$. It can be seen that the on-site energy varies for distinct lattice sites mimicking a random potential. Actually, the parameter s_2 just scales the disorder and thus our considerations are valid for arbitrary disorder strength ϵ^* . To evaluate a histogram of the energy distribution we subtract the disordered potential at the lattice sites from the pure potential and shift the difference by its mean ϵ^* . This yields a distribution which is centered around zero. The shift could have been absorbed as well in the definition of the chemical potential μ . The histogram for 2048 lattice sites is shown in Fig. 7. In the center the distribution is rather flat, yet, there are important fea-

tures at the boundary. Such a distribution can be well described by a shifted β distribution.

The β distribution $q_\beta(u|a, b)$, which is defined on the interval $u \in [0, 1]$, is given by

$$q_\beta(u|a, b) \equiv \frac{1}{B(a, b)} u^{a-1} (1-u)^{b-1},$$

where

$$B(a, b) = \int_0^1 dp p^{a-1} (1-p)^{b-1} = \frac{\Gamma(a)\Gamma(b)}{\Gamma(a+b)}.$$

The expectation value of $q_\beta(u|a, b)$ is

$$\langle u \rangle = \frac{a}{a+b} \quad (\text{A1})$$

and its variance is

$$\text{var}(u) = \frac{\langle u \rangle (1 - \langle u \rangle)}{a + b + 1}. \quad (\text{A2})$$

To obtain a distribution which is symmetric around zero and bounded by $[-1, 1]$ we set $\langle u \rangle = 0.5$, shift the whole β distribution by this value and scale it by a factor of 2. Resolving Eqs. (A1) and (A2) under the condition that $\langle u \rangle = 0.5$ leads to $a = b = [\text{var}(u)/4 - 1]/2$. For $\text{var}(u) > 1/12$ (where $1/12$ is the variance of the uniform distribution), the probability density is shifted toward the boundaries of the distribution. In particular we set $\text{var}(u) = 0.12$. Finally, we draw 2048 samples from this specific shifted β distribution, which we denote as $q(\epsilon_i/\epsilon^*)$. The resulting distribution of the 2048 samples is indicated by the solid line in Fig. 7, which reproduces well the distribution obtained from the experiment with two incommensurate optical lattices.

-
- [1] M. P. A. Fisher, P. B. Weichman, G. Grinstein, and D. S. Fisher, *Phys. Rev. B* **40**, 546 (1989).
- [2] P. A. Crowell, F. W. Van Keuls, and J. D. Reppy, *Phys. Rev. Lett.* **75**, 1106 (1995).
- [3] G. A. Csáthy, J. D. Reppy, and M. H. W. Chan, *Phys. Rev. Lett.* **91**, 235301 (2003).
- [4] D. B. Haviland, Y. Liu, and A. M. Goldman, *Phys. Rev. Lett.* **62**, 2180 (1989).
- [5] H. S. J. van der Zant, W. J. Elion, L. J. Geerligs, and J. E. Mooij, *Phys. Rev. B* **54**, 10081 (1996).
- [6] D. Jaksch, C. Bruder, J. I. Cirac, C. W. Gardiner, and P. Zoller, *Phys. Rev. Lett.* **81**, 3108 (1998).
- [7] I. Bloch, J. Dalibard, and W. Zwerger, *Rev. Mod. Phys.* **80**, 885 (2008).
- [8] M. Greiner, O. Mandel, T. Esslinger, T. W. Hänsch, and I. Bloch, *Nature (London)* **415**, 39 (2002).
- [9] A. Aspect and M. Inguscio, *Physics Today* **62**, 30 (2009).
- [10] L. Fallani, J. E. Lye, V. Guarrera, C. Fort, and M. Inguscio, *Phys. Rev. Lett.* **98**, 130404 (2007).
- [11] R. Roth and K. Burnett, *Phys. Rev. A* **68**, 023604 (2003).
- [12] B. Damski, J. Zakrzewski, L. Santos, P. Zoller, and M. Lewenstein, *Phys. Rev. Lett.* **91**, 080403 (2003).
- [13] M. Hild, F. Schmitt, and R. Roth, *J. Phys. B* **39**, 4547 (2006).
- [14] F. Schmitt, M. Hild, and R. Roth, *Phys. Rev. A* **80**, 023621 (2009).
- [15] M. Pasienski, D. McKay, M. White, and B. DeMarco, *Nat. Phys.* **6**, 677 (2010).
- [16] M. White, M. Pasienski, D. McKay, S. Q. Zhou, D. Ceperley, and B. DeMarco, *Phys. Rev. Lett.* **102**, 055301 (2009).
- [17] J. E. Lye, L. Fallani, M. Modugno, D. S. Wiersma, C. Fort, and M. Inguscio, *Phys. Rev. Lett.* **95**, 070401 (2005).
- [18] U. Shrestha and M. Modugno, *Phys. Rev. A* **82**, 033604 (2010).
- [19] S. Ospelkaus, C. Ospelkaus, O. Wille, M. Succo, P. Ernst, K. Sengstock, and K. Bongs, *Phys. Rev. Lett.* **96**, 180403 (2006).
- [20] R. T. Scalettar, G. G. Batrouni, and G. T. Zimanyi, *Phys. Rev. Lett.* **66**, 3144 (1991).
- [21] W. Krauth, N. Trivedi, and D. Ceperley, *Phys. Rev.*

- Lett. **67**, 2307 (1991).
- [22] K. Sheshadri, H. R. Krishnamurthy, R. Pandit, and T. V. Ramakrishnan, Phys. Rev. Lett. **75**, 4075 (1995).
- [23] J. K. Freericks and H. Monien, Phys. Rev. B **53**, 2691 (1996).
- [24] B. V. Svistunov, Phys. Rev. B **54**, 16131 (1996).
- [25] J. Kisker and H. Rieger, Phys. Rev. B **55**, R11981 (1997).
- [26] I. F. Herbut, Phys. Rev. Lett. **79**, 3502 (1997).
- [27] N. Prokof'ev and B. Svistunov, Phys. Rev. Lett. **92**, 015703 (2004).
- [28] K. G. Balabanyan, N. Prokof'ev, and B. Svistunov, Phys. Rev. Lett. **95**, 055701 (2005).
- [29] P. Buonsante, V. Penna, A. Vezzani, and P. B. Blakie, Phys. Rev. A **76**, 011602 (2007).
- [30] P. B. Weichman and R. Mukhopadhyay, Phys. Rev. B **77**, 214516 (2008).
- [31] L. Pollet, N. V. Prokof'ev, B. V. Svistunov, and M. Troyer, Phys. Rev. Lett. **103**, 140402 (2009).
- [32] V. Gurarie, L. Pollet, N. V. Prokof'ev, B. V. Svistunov, and M. Troyer, Phys. Rev. B **80**, 214519 (2009).
- [33] U. Bissbort and W. Hofstetter, Europhys. Lett. **86**, 50007 (2009).
- [34] F. Krüger, J. Wu, and P. Phillips, Physical Review B **80**, 094526 (2009).
- [35] F. Krüger, S. Hong, and P. Phillips, arXiv:1006.2395 (2010).
- [36] D. Clément, N. Fabbri, L. Fallani, C. Fort, and M. Inguscio, Phys. Rev. Lett. **102**, 155301 (2009).
- [37] N. Fabbri, D. Clément, L. Fallani, C. Fort, M. Modugno, K. M. R. van der Stam, and M. Inguscio, Phys. Rev. A **79**, 043623 (2009).
- [38] P. T. Ernst, S. Gotze, J. S. Krauser, K. Pyka, D. Luhmann, D. Pfannkuche, and K. Sengstock, Nat Phys **6**, 56 (2010).
- [39] D. Clément, N. Fabbri, L. Fallani, C. Fort, and M. Inguscio, New J. Phys. **11**, 103030 (2009).
- [40] D. Clément, N. Fabbri, L. Fallani, C. Fort, and M. Inguscio, J. Low Temp. Phys. **158**, 5 (2010).
- [41] W. Zwerger, Journal of Optics B: Quantum and Semi-classical Optics **5**, S9 (2003).
- [42] M. Potthoff, M. Aichhorn, and C. Dahnken, Phys. Rev. Lett. **91**, 206402 (2003).
- [43] D. Clément, A. F. Varón, J. A. Retter, L. Sanchez-Palencia, A. Aspect, and P. Bouyer, New J. Phys. **8**, 165 (2006).
- [44] S. Q. Zhou and D. M. Ceperley, Phys. Rev. A **81**, 013402 (2010).
- [45] W. Koller and N. Dupuis, J. Phys.: Condens. Matter **18**, 9525 (2006).
- [46] M. Aichhorn, M. Hohenadler, C. Tahan, and P. B. Littlewood, Phys. Rev. Lett. **100**, 216401 (2008).
- [47] M. Knap, E. Arrigoni, and W. von der Linden, Phys. Rev. B **81**, 024301 (2010).
- [48] M. Potthoff and M. Balzer, Phys. Rev. B **75**, 125112 (2007).
- [49] M. Aichhorn, E. Arrigoni, M. Potthoff, and W. Hanke, Phys. Rev. B **74**, 235117 (2006).
- [50] M. G. Zacher, R. Eder, E. Arrigoni, and W. Hanke, Phys. Rev. B **65**, 045109 (2002).
- [51] M. Potthoff, Eur. Phys. J. B **32**, 429 (2003).
- [52] M. Potthoff, Eur. Phys. J. B **36**, 335 (2003).
- [53] M. Knap, E. Arrigoni, and W. von der Linden, Phys. Rev. B **81**, 235122 (2010).
- [54] T. Stöferle, H. Moritz, C. Schori, M. Köhl, and T. Esslinger, Phys. Rev. Lett. **92**, 130403 (2004).
- [55] A. Albuquerque, F. Alet, P. Corboz, P. Dayal, A. Feiguin, S. Fuchs, L. Gamper, E. Gull, S. Gürtler, A. Honecker, R. Igarashi, M. Körner, A. Kozhevnikov, A. Läuchli, S. Manmana, M. Matsumoto, I. McCulloch, F. Michel, R. Noack, G. Pawłowski, L. Pollet, T. Pruschke, U. Schollwöck, S. Todo, S. Trebst, M. Troyer, P. Werner, S. Wessel, and for the ALPS collaboration, J. Magn. Mater. **310**, 1187 (2007).